The Astrophysical Journal, 657: L117–L120, 2007 March 10

ISOTOPIC FRACTIONATION OF NITROGEN IN AMMONIA IN THE TROPOSPHERE OF JUPITER

Mao-Chang Liang,[1,2] Bing-Ming Cheng,[3] Hsiao-Chi Lu,[3] Hong-Kai Chen,[3]
M. S. Alam,[3] Yuan-Pern Lee,[4] and Yuk L. Yung[2]
Received 2006 November 11; accepted 2007 January 29; published 2007 February 21

ABSTRACT

Laboratory measurements of the photoabsorption cross section of $^{15}NH_3$ at wavelengths between 140 and 220 nm are presented for the first time. Incorporating the measured photoabsorption cross sections of $^{15}NH_3$ and $^{14}NH_3$ into a one-dimensional photochemical diffusive model, we find that at 400 mbar, the photolytic efficiency of $^{15}NH_3$ is about 38% greater than that of $^{14}NH_3$. In addition, it is known that ammonia can condense in the region between 200 and 700 mbar, and the condensation tends to deplete the abundance ratio of $^{15}NH_3$ and $^{14}NH_3$. By matching the observed ratio of $^{15}NH_3$ and $^{14}NH_3$ at 400 mbar, the combined effect of photolysis and microphysics produces the ratio of $(2.42 \pm 0.34) \times 10^{-3}$ in the deep atmosphere, in excellent agreement with the *Galileo* spacecraft measurements. The usefulness of the isotopic composition of ammonia as a tracer of chemical and dynamical processes in the troposphere of Jupiter is discussed.

Subject headings: atmospheric effects — planetary systems — planets and satellites: individual (Jupiter) — radiative transfer

1. INTRODUCTION

Ammonia can condense to form ammonia ice at 720 mbar for the solar N/H ratio, 840 mbar for 3 times solar N/H, or 1000 mbar for 4 times solar N/H (Atreya & Wong 2005; Atreya et al. 2005). The N/H ratio in the deep atmosphere of Jupiter is constrained to be 3–4 times solar abundance (Folkner et al. 1998; Atreya et al. 2003; Wong et al. 2004), setting the condensation level to be at ~900 mbar. Condensation processes usually preferentially select heavier isotopologues. Photolysis can either enhance (e.g., see Cheng et al. 2006; Liang et al. 2004) or deplete (e.g., $^{15}NH_3$, this work; $OC^{34}S$, Leung et al. 2002) the abundance of heavy isotopologues. So the isotopic composition of molecules provides a tool for understanding chemical and dynamical processes in the atmospheres of planets. For example, the highly depleted D/H ratio in HDO and H_2O in the upper atmosphere of Mars (Krasnopolsky et al. 1998) can be satisfactorily explained by condensation/evaporation (Bertaux & Montmessin 2001) and photolytic processes (Cheng et al. 1999).

The $^{15}N/^{14}N$ isotopic ratio in the atmosphere of Jupiter has been determined by various groups (Encrenaz et al. 1978; Tokunaga et al. 1980; Fouchet et al. 2000, 2004; Owen et al. 2001; Abbas et al. 2004). The observed $^{15}N/^{14}N$ ratios in ammonia at ~400 mbar from the *Infrared Space Observatory* Short Wavelength Spectrometer (Fouchet et al. 2000) and *Cassini* spacecraft Composite Infrared Spectrometer (Abbas et al. 2004; Fouchet et al. 2004) are, respectively, $1.9^{+0.9}_{-1.0} \times 10^{-3}$ and $(2.23 \pm 0.31) \times 10^{-3}$. In the deeper atmosphere somewhere between 0.9 and 2.9 bar, the in situ *Galileo* Probe Mass Spectrometer (GPMS) returned a value of $(2.3 \pm 0.3) \times 10^{-3}$ (Owen et al. 2001), similar to that at higher altitudes. These values are a factor of ~2 less than the terrestrial value 3.68×10^{-3} and the cometary (Hale-Bopp) value of $3.1^{+0.5}_{-0.4} \times 10^{-3}$ (Jewitt et al. 1997). Recently from the solar wind record of nitrogen archived on the Moon, Hashizume et al. (2000) found that $^{15}N/^{14}N$ is depleted by at least 24% (or the ratio $\lesssim 2.8 \times 10^{-3}$) relative to the terrestrial value. From the *Solar and Heliospheric Observatory*, Kallenbach et al. (1998) directly measured the $^{15}N/^{14}N$ ratio in the solar wind to be $5.0^{+1.7}_{-1.0} \times 10^{-3}$. The ratio is found to be $(2.2 \pm 0.5) \times 10^{-3}$ in the local interstellar medium (Dahmen et al. 1995) and $\sim 10^{-2}$ in the Large Magellanic Cloud (Chin et al. 1999). It is important to note that the ratio could be very different between molecules (e.g., Hutsemekers et al. 2005). The observed depleted abundance of $^{15}NH_3$ in the troposphere of Jupiter (relative to the terrestrial value) leads Owen and colleagues (e.g., Owen et al. 2001; Owen & Encrenaz 2003) to propose that the tropospheric $^{15}N/^{14}N$ can be used to indicate the solar nebula value.

In this Letter, we investigate the ammonia isotope ratio by considering the photolytic processes of ammonia, based on the laboratory measured photoabsorption cross sections of NH_3 and its isotopologues, in the troposphere of Jupiter.

2. MEASUREMENTS OF PHOTOABSORPTION CROSS SECTIONS FOR $^{15}NH_3$ AND $^{14}NH_3$

The photoabsorption cross sections (Fig. 1) for $^{15}NH_3$ and $^{14}NH_3$ in the wavelengths between ~140 and 230 nm are measured at a spectral resolution of 0.02 nm, using vacuum ultraviolet light produced in the National Synchrotron Radiation Research Center in Taiwan.[5] The spectral range is associated with two transitions: $A \leftarrow X$ (~165–200 nm) and $B \leftarrow X$ (~140–170 nm). To our knowledge, the absorption cross sections of $^{15}NH_3$ are new. Considering all possible systematic errors, experimental uncertainties of cross sections are estimated to be within 10% of reported values. See Cheng et al. (2006) for experimental details.

The absorption maxima in the $A \leftarrow X$ transition of $^{15}NH_3$ are redshifted from those of $^{14}NH_3$ by ~0.02 nm for the vibrational band $v' = 0$; the shifts increase gradually to 0.24 nm for $v' = 13$. The widths for the corresponding vibrational bands of $^{15}NH_3$ and $^{14}NH_3$ are similar. The maximal absorption cross sections of

[1] Research Center for Environmental Changes, Academia Sinica, Taipei 115, Taiwan; mcl@rcec.sinica.edu.tw.
[2] Division of Geological and Planetary Sciences, California Institute of Technology, Pasadena, CA 91125; yly@gps.caltech.edu.
[3] National Synchrotron Radiation Research Center, Hsinchu Science Park, Hsinchu 30076, Taiwan; bmcheng@nsrrc.org.tw.
[4] Department of Applied Chemistry and Institute of Molecular Science, National Chiao Tung University, Hsinchu 30010, Taiwan; yplee@mail.nctu.edu.tw.

[5] Digitized cross sections at 0.02 nm spectral resolution are available at http://ams-bmc.nsrrc.org.tw.

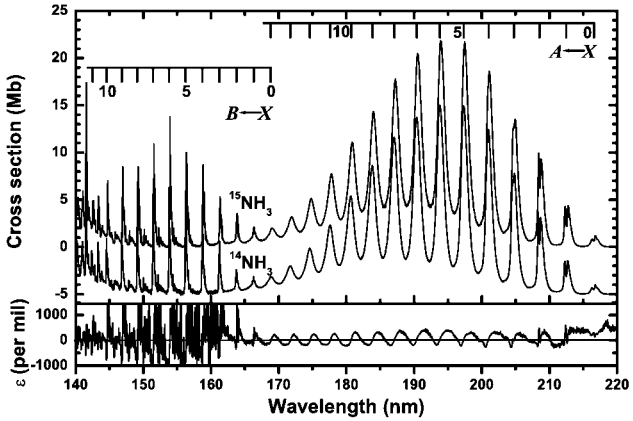

FIG. 1.—*Top*: Absorption cross sections (in units of megabarn, 1 Mbarn = 10^{-18} cm^2) in the spectral region 140–220 nm for $^{15}NH_3$ and $^{14}NH_3$. For best visualization, the cross section of $^{14}NH_3$ is offset by −5 Mbarn. *Bottom*: Fractionation factor (ϵ) of $^{15}NH_3$, defined by $1000(\sigma/\sigma_0 - 1)$, where σ and σ_0 are the cross sections of $^{15}NH_3$ and $^{14}NH_3$, respectively. See Liang et al. (2004) for details of ϵ factor.

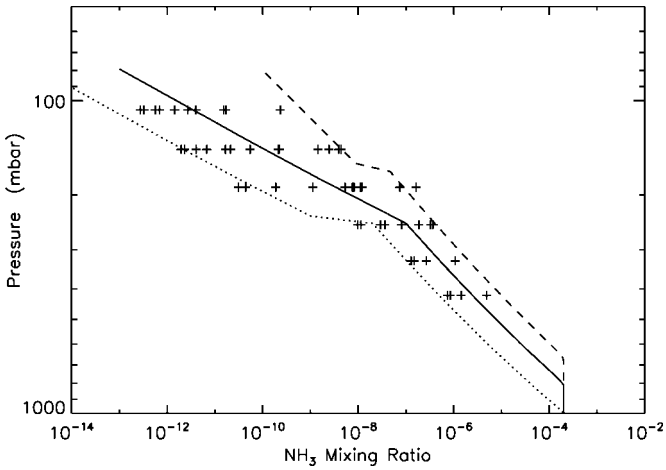

FIG. 2.—Vertical profile of NH_3 (*solid line*) used in the model. Crosses are measurements by Edgington et al. (1999). Dashed and dotted lines represent an upper and lower bound of measured NH_3 mixing ratios, respectively. The profiles used in this study are consistent with that obtained by Fouchet et al. (2000).

this transition of $^{15}NH_3$ are greater than those of $^{14}NH_3$ by 15%–23% for the first three vibrational bands and by 5%–9% for the other bands. Similarly, the absorption maxima of bands in the $B \leftarrow X$ transition of $^{15}NH_3$ are redshifted from those of $^{14}NH_3$ by 0.08–0.24 nm; the widths for the vibrational bands of $^{15}NH_3$ are slightly smaller than the corresponding bands of $^{14}NH_3$. However, the behavior of the maxima for absorption cross sections of $^{15}NH_3$ and $^{14}NH_3$ in the $B \leftarrow X$ transition is different from that in the $A \leftarrow X$ transition; those of $^{15}NH_3$ increase by 6%–40% for bands $v' = 0$–2 relative to those of $^{14}NH_3$ and 3%–29% for bands $v' = 6$–11 but decrease by 3%–6% for bands $v' = 3$–5.

The oscillator strength (Herzberg 1950) f is defined by $1.13 \times 10^{-6} \int \sigma \, d\nu$, where σ is the cross section in megabarns ($=10^{-18}$ cm^2) and ν is the wavenumber (cm^{-1}). The value of f integrated over 165–220 nm for the $A \leftarrow X$ transition of $^{15}NH_3$ is 0.00858, only 7.3% greater than that (0.0800) of $^{14}NH_3$ in the $A \leftarrow X$ transition. Although absorption maxima and bandwidths of the $A \leftarrow X$ transition for all four deuterated $^{14}NH_3$ isotopologues varied substantially with the number of D (^{2}H) atoms in each isotopologue, their f-values are almost identical (Cheng et al. 2006). For the $B \leftarrow X$ transition of $^{15}NH_3$, the value of f integrated over 144–165 nm is 0.0104, 16% smaller than the value of 0.0124 for $^{14}NH_3$. We also observed similarly large variations of f-values for $B \leftarrow X$ transitions among four deuterated isotopologues of NH_3 in the previous work (Cheng et al. 2006). For instance, the f-values of $^{14}NH_2D$ and $^{14}ND_3$ are smaller than that of $^{14}NH_3$ by 23%–27%. Thus, the $B \leftarrow X$ transition is affected by vibrational excitation, presumably due to vibronic coupling (Lin 1976; Liao et al. 1999).

The shift of band origin between isotopologues reflects the difference in zero-point energy of the excited and ground states for these species. The absorption maximum (216.76 nm) of $v' = 0$ in the $A \leftarrow X$ transition of $^{15}NH_3$ is redshifted from that of $^{14}NH_3$ by only 0.02 nm, or -4 cm^{-1}. In contrast, the shifts between four deuterated isotopologues of NH_3 are 0.80, 0.82, and 0.85 nm to the blue for each increase in the number of D atoms, or 171, 176, and 185 cm^{-1}. Notably, other vibrational bands of $^{15}NH_3$ in A state are all redshifted from those of $^{14}NH_3$, whereas those of the three deuterated isotopologues of NH_3 are all blueshifted. According to calculations (McCarthy et al. 1987; Cheng et al. 2006), the A state of NH_3 dissociates into NH_2 ($^2B_1$) + H with a small barrier. Because the solar flux decreases rapidly as the wavelength decreases in this spectral region, we expect that the isotopic photo-induced fractionation has opposite effects for D- and ^{15}N-isotopologues. The fractionation factor of $^{15}NH_3$ is presented in the lower panel of Figure 1. The figure shows that enhanced photolysis of $^{15}NH_3$ occurs at wavelengths greater than ~210 nm.

3. MODEL DESCRIPTION AND SIMULATION RESULTS

By analogy with mechanisms that fractionate the isotopic composition of water in the atmosphere of Mars (Bertaux & Montmessin 2001), we consider photolysis and condensation processes of ammonia in the troposphere of Jupiter. We first calculate the isotopic fractionation of ammonia due to photolysis, and one-dimensional models are sufficient for such purpose. The one-dimensional Caltech/JPL KINETICS model is used in our study. A detailed description of the model has been given elsewhere (e.g., Gladstone et al. 1996; Moses et al. 2005). Due to the complexity of chemical and (micro)physical processes involving ammonia, we fix the vertical profiles of ammonia based on the observations (e.g., Edgington et al. 1999) and defer self-consistent modeling (dynamics, microphysics, and photochemistry coupled calculation) to a later paper. The vertical profile of ammonia is shown by the solid line in Figure 2, which is the same as the one used in a companion paper (Cheng et al. 2006); this is set to be the reference profile.

Because of absorption by CH_4 and C_2H_6 in the upper atmosphere of Jupiter, UV photons at wavelengths shorter than ~160 nm are absent in the troposphere (Gladstone et al. 1996; Moses et al. 2005). The measured photoabsorption cross sections for ammonia isotopologues (Fig. 1) between 140 and 230 nm are suitable for our investigation in the troposphere. The photoabsorption of ammonia mostly takes place in the region between ~200 and 700 mbar (see Fig. 3, *dashed line*), covering the region of interest at ~400 mbar.

The photolytic efficiencies of $^{15}NH_3$ and $^{14}NH_3$ are shown in Figure 3. Over the region of interest, the photolysis of $^{15}NH_3$ prevails, resulting in a depletion of the abundance of $^{15}NH_3$ ($[^{15}NH_3]$). The column-integrated photolysis rate of ammonia is ~10^{12} molecules cm^{-2} s^{-1} and is insensitive to the prescribed ammonia vertical profiles. We define $\beta = J(^{15}NH_3)/J(^{14}NH_3)$,

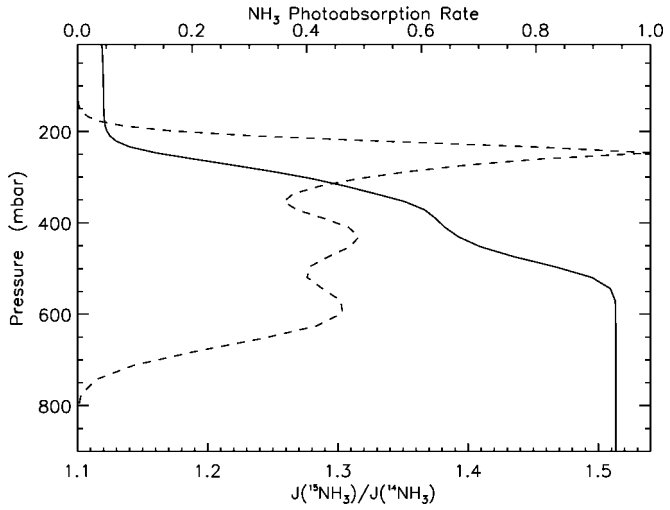

FIG. 3.—Vertical profile of β, the ratio (*solid line*) of the J (photolysis rate coefficient) values of $^{14}NH_3$ and $^{15}NH_3$ in the atmosphere of Jupiter, calculated using the reference ammonia profile (Fig. 2, *solid line*). The photoabsorption rate of NH_3 is overplotted by a dashed line using the cross section presented in Fig. 1. The maximum rate (1.0) corresponds to 9.1×10^5 molecules cm^{-3} s^{-1}.

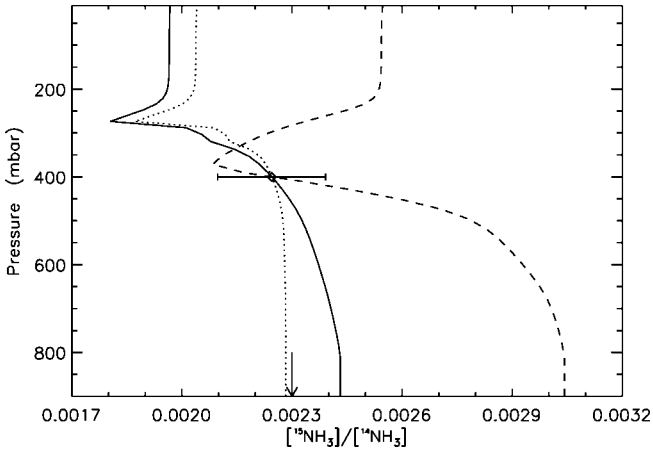

FIG. 4.—Vertical profile of $[^{15}NH_3]/[^{14}NH_3]$, obtained by matching the *Cassini* measurement (Abbas et al. 2004) at 400 mbar, represented by the diamond with the reported one-σ statistical error bar. Calculations coupled with ammonia photolysis and microphysics processes are represented by the solid line. For comparison, results that only consider photolysis and vertical mixing processes are shown by the dotted line. The arrow indicates the *Galileo* GPMS measurements (Owen et al. 2001) in the deep atmosphere. The dashed line denotes a sensitivity study to the changes of ammonia condensation rates based on the vertical eddy mixing coefficients used by Gladstone et al. (1996). See text for details.

where J is the photolysis rate coefficient, and $\gamma = ([^{15}NH_3]/[^{14}NH_3])/([^{15}NH_3]_0/[^{14}NH_3]_0)$, where $[^{15}NH_3]_0$ and $[^{14}NH_3]_0$ are the abundances of $^{15}NH_3$ and $^{14}NH_3$ in the deep atmosphere, respectively. The γ in photochemical equilibrium equals $1/\beta$. At 400 mbar, $\beta = 1.38$. This implies $\gamma = 72.5\%$. Below the ~550 mbar altitude level, our model shows $\gamma = 66\%$. In contrast, $^{14}NH_2D$ shows an enrichment of the abundance above 450 mbar level and depletion below (Cheng et al. 2006). The γ value for $^{14}NH_2D$ has a maximum of 143.9% at 300 mbar and levels off at a value about 70% below ~550 mbar level. Note that the above calculations are based on photochemical equilibrium arguments. See, for example, Yung et al. (1997) and Liang et al. (2007) for an in-depth discussion on the isotopic composition of species in photochemical equilibrium and the role of dynamics in modifying photochemical effects.

Varying the concentration profiles of NH_3 can modify the results presented above. For this, we change the NH_3 profiles shown in Figure 2. With lower NH_3 abundance (*dotted line*), $\gamma = 76.5\%$ ($\beta = 1.31$) at 400 mbar. For higher NH_3 abundance (*dashed line*), $\gamma = 66.6\%$ ($\beta = 1.50$). All these sensitivity studies give $\gamma = 72\% \pm 5\%$. From the *Cassini* measured $[^{15}NH_3]/[^{14}NH_3] = (2.23 \pm 0.31) \times 10^{-3}$, $[^{15}NH_3]_0/[^{14}NH_3]_0 = (3.10 \pm 0.48) \times 10^{-3}$ is inferred. This value is greater than the GPMS value of $(2.3 \pm 0.3) \times 10^{-3}$ below 0.9 bar level, where the photolysis-induced fractionation is negligible (see Fig. 3), although the difference is not significant. However, the FWHM of the contribution function of the observations (e.g., see Fouchet et al. 2004) is as wide as the region where the photolytic process of ammonia is important; the total column photolysis rate of ammonia would be a better indicator to represent the photochemical effect of ammonia. The column integrated $\beta = 1.323$ and $\gamma = 75.6\%$; the values are insensitive to the selection of ammonia vertical profiles. The implied $[^{15}NH_3]_0/[^{14}NH_3]_0$ is $(2.95 \pm 0.41) \times 10^{-3}$, close to the value calculated at 400 mbar. So 400 mbar level is selected for the following discussion.

The microphysical processes of ammonia and vertical eddy mixing can also affect the isotopic composition of ammonia. Following the same method as that by Fouchet et al. (2000) and Bertaux & Montmessin (2001), we can express γ as $[X(NH_3)/X(NH_{3,0})]^{\alpha-1}$, where $X(NH_3)$ and $X(NH_{3,0})$ are the volume mixing ratios at higher altitudes and in the deep atmosphere, respectively. The fractionation coefficient α is determined experimentally. Since the ammonia condensation rate has not been calculated/measured, we estimate the rate based on the ammonia mixing ratio profile prescribed by the solid line in Figure 2 and the eddy mixing coefficients from Moses et al. (2005) based on Edgington et al. (1999) observations. Assuming $X(NH_{3,0}) = 2 \times 10^{-4}$ (e.g., Abbas et al. 2004), we find that ammonia can condense in the region between ~300 and 800 mbar. The lower and upper limits are set by photolysis and and saturation relation of NH_3, respectively. Over the ~300 and 800 mbar region, the ammonia microphysics process is more important than the photolysis, resulting in the dilution of the depletion of ^{15}N caused by photolysis (see Fig. 4). Applying the α measured for the liquid-vapor transition of $^{15}NH_3$ (Thode 1940; Jancso & van Hook 1974), we obtain $\gamma = 92.3\%$ at 400 mbar and infer $[^{15}NH_3]_0/[^{14}NH_3]_0 = (2.42 \pm 0.34) \times 10^{-3}$, in excellent agreement with the GPMS measurements. Note that the α used in the above calculation is extrapolated from the values measured at higher temperature (~195–240 K vs. 130 K for the region of interest in Jupiter).

The above estimation of the isotopic fractionation of ammonia due to ammonia condensation is calculated by assuming the "open" cloud system, where the condensed phase is in isotopic equilibrium with the vapor phase and the condensed particles leave the system immediately after their formation. There is another model that results in smaller isotopic fractionation: the "closed" cloud model, in which the condensed and vapor phases stay in the same air parcel. See, for example, Fouchet & Lellouch (2000) for a detailed description of the two models. The latter model gives $[^{15}NH_3]_0/[^{14}NH_3]_0 = (2.27 \pm 0.32) \times 10^{-3}$.

To estimate the sensitivity of the results to the changes of vertical eddy mixing coefficients, a case based on the Gladstone et al. (1996) eddy profile is shown by the dashed line in Figure 4; the tropospheric eddy mixing coefficient in this case is 10^3 cm^2 s^{-1}, a factor of 10 less than that (~10^4 cm^2 s^{-1}) used by Moses et al. (2005). In this case, the inferred $[^{15}NH_3]_0/[^{14}NH_3]_0 = 3.02 \times 10^{-3}$, suggesting that vertical transport plays a crucial role in the vertical profiles of the nitrogen isotopic composition of ammonia.

In contrast, the abundance of NH_2D is less affected (<10%) by the selection of vertical eddy mixing coefficients. The main reason for this is that the microphysical processes dominate the isotopic fractionation in NH_2D.

To test the above estimation of the ammonia condensation rate, we perform a microphysics calculation using the Community Aerosol and Radiation Model for Atmospheres (CARMA; Toon et al. 1988). We find that at ~400 mbar, the ammonia ice production rate ranges between $<1 \times 10^{-15}$ and 9×10^{-12} g cm^{-3} s^{-1} (relative humidity ~100%–120%), obtained over a variety of initial conditions (i.e., mean radius of condensation nuclei of 0.01–0.5 μm, number of condensation nuclei of 0.1–100 cm^{-3}, and initial relative humidity of NH_3 of 100%–300%), which could be much greater than the nominal production rate (~10^{-16} g cm^{-3} s^{-1}) used in Figure 4, suggesting that the microphysical processes of ammonia could be more efficient than we expect from vertical eddy mixing processes to homogenize the isotopic composition of ammonia between 400 mbar level and lower altitudes.

4. DISCUSSION AND SUMMARY

Elemental and isotopic measurements provide a wealth of information for the formation and evolution of the solar system. The currently favored formation scenario for giant planets suggests that heavier elements are enriched compared with the solar or protosolar abundances. The degree of enrichments (roughly by a factor of 3 ± 1, compared with solar abundances, for Jupiter) represents the fraction of core mass to the surrounding gaseous envelope (Mizuno 1980; Pollack et al. 1996), as well as the conditions such as temperature for trapping these elements in the icy planetesimals for the formation of giant planets (e.g., Owen & Encrenaz 2003). Molecular nitrogen is the biggest N reservoir in solar nebulae. However, it is so volatile that it can hardly be incorporated into planets during their formation. Ammonia is likely to be the major N carrier in giant planets. It has been shown that ion-molecule reactions (Terzieva & Herbst 2000) in interstellar clouds could enrich $^{15}N/^{14}N$ in HCN relative to N_2. Yet the observed $^{15}N/^{14}N$ for Jupiter smaller than that for the comet Hale-Bopp leads Owen et al. (2001) to suggest that the measured $^{15}N/^{14}N$ in ammonia represents the protosolar value. In contrast, our calculation suggests that the inferred $^{15}N/^{14}N$ in the lower atmosphere of Jupiter could be modified by the photolytic processes of ammonia above ~700 mbar level.

We demonstrate that vertical eddy mixing coefficients at and below 400 mbar altitude level $\gg 10^3$ cm^2 s^{-1} can greatly dilute the ammonia photolytic effect. No evident latitudinal variation of $^{15}N/^{14}N$ in ammonia was found (Abbas et al. 2004), suggesting that the ammonia abundances at 400 mbar at latitudes between $\pm 40°$ are controlled primarily by the microphysics of ammonia. The formation of ice particles followed by dynamical processes such as convection (Gierasch et al. 2000; Ingersoll et al. 2000) provides an alternative explanation to the observed $^{15}NH_3/^{14}NH_3$ at 400 mbar and in the deep atmosphere; the evaporation of ammonia ice supplies the loss of ammonia due to photolysis. Further modeling coupled with photochemistry, dynamics, and microphysics could provide valuable information for the dynamical properties in the troposphere of Jupiter. The isotopic composition measurements of NH_2D and $^{15}NH_3$ at various altitudes and latitudes will be needed to constrain model parameters (e.g., atmospheric dynamics). Laboratory measurements of the photoabsorption cross sections of ammonia isotopologues and fractionation coefficients (α) due to condensation at lower temperature (~150 K) are required to refine our calculation.

We thank Geoff Blake and John Eiler for helpful discussion, and Andy Ackerman, Xin Guo, Run-Lie Shia, and Giovanna Tinetti for assisting the CARMA simulation, and Chris Parkinson for useful comments. Special thanks are due the referee Emmanuel Lellouch for his insightful comments. This work was supported by NASA grant NNG06GF33G to the California Institute of Technology. B.-M. C. was supported by the National Science Council of Taiwan (grant NSC95-2113-M-213-006).

REFERENCES

Abbas, M. M., et al. 2004, ApJ, 602, 1063
Atreya, S. K., Mahaffy, P. R., Niemann, H. B., Wong, M. H., & Owen, T. C. 2003, Planet. Space Sci., 51, 105
Atreya, S. K., & Wong, A. S. 2005, Space Sci. Rev., 116, 121
Atreya, S. K., Wong, A. S., Baines, K. H., Wong, M. H., & Owen, T. C. 2005, Planet. Space Sci., 53, 498
Bertaux, J.-L., & Montmessin, F. 2001, J. Geophys. Res., 106, 32879
Cheng, B.-M., Chew, E. P., Liu, C.-P., Bahou, M., Lee, Y.-P., Yung, Y. L., & Gerstell, M. F. 1999, Geophys. Res. Lett., 26, 3657
Cheng, B.-M, Lu, H.-C., Chen, H.-K., Bahou, M., Lee, Y.-P., Mebel, A. M., Liang, M.-C., & Yung, Y. L. 2006, ApJ, 647, 1535
Chin, Y. N., Henkel, C., Langer, N., & Mauersberger, R. 1999, ApJ, 512, L143
Dahmen, G., Wilson, T. L., & Matteucci, F. 1995, A&A, 295, 194
Edgington, S. G., Atreya, S. K., Trafton, L. M., Caldwell, J. J., Beebe, R. F., Simon, A. A., & West, R. A. 1999, Icarus, 142, 342
Encrenaz, T., Combes, M., & Zeau, Y. 1978, A&A, 70, 29
Folkner, W. M., Woo, R., & Nandi, S. 1998, J. Geophys. Res., 103, 22847
Fouchet, T., Irwin, P. G. J., Parrish, P., Calcutt, S. B., Taylor, F. W, Nixon, C. A., & Owen, T. 2004, Icarus, 172, 50
Fouchet, T., & Lellouch, E. 2000, Icarus, 144, 114
Fouchet, T., Lellouch, E., Bezard, B., Encrenaz, T., Drossart, P., Feuchtgruber, H., & de Graauw, T. 2000, Icarus, 143, 223
Gierasch, P. J., et al. 2000, Nature, 403, 628
Gladstone, G. R., Allen, M., & Yung, Y. L. 1996, Icarus, 119, 1
Hashizume, K., Chaussidon, M., Marty, B., & Robert, F. 2000, Science, 290, 1142
Herzberg, G. 1950, Molecular Spectra and Molecular Structure I (New York: Van Nostrand)
Hutsemekers, D., Manfroid, J., Jehin, E., Arpigny, C., Cochran, A., Schulz, R., Stuwe, J. A., & Zucconi, J. M. 2005, A&A, 440, L21
Ingersoll, A. P., Gierasch, P. J., Banfield, D., & Vasavada, A. R. 2000, Nature, 403, 630
Jancso, G., & van Hook, W. A. 1974, Chem. Rev., 74, 689
Jewitt, D. C., Matthews, H. E., Owen, T., & Meier, R. 1997, Science, 278, 90
Kallenbach, R., et al. 1998, ApJ, 507, L185
Krasnopolsky, V. A., Mumma, M. J., & Gladstone, G. R. 1998, Science, 280, 1576
Leung, F. Y. T., Colussi, A. J., Hoffmann, M. R., & Toon, G. C. 2002, Geophys. Res. Lett., 29, 112
Liang, M.-C., Blake, G. A., Lewis, B. R., & Yung, Y. L. 2007, Proc. Natl. Acad. Sci., 104, 21
Liang, M.-C., Blake, G. A., & Yung, Y. L. 2004, J. Geophys. Res., 109, D10308
Liao, D.-W., Mebel, A. M., Hayashi, M., Shiu, Y. J., Chen, Y.-T., & Lin, S. H. 1999, J. Chem. Phys., 111, 205
Lin, S. H. 1976, Proc. R. Soc. London A, 352, 57
McCarthy, M. I., Rosmus, P., Werner, H.-J., Botschwina, P., & Vaida, V. 1987, J. Chem. Phys., 86, 6693
Mizuno, H. 1980, Prog. Theor. Phys., 64, 544
Moses, J. I., Fouchet, T., Bezard, B., Gladstone, G. R., Lellouch, E., & Feuchtgruber, H. 2005, J. Geophys. Res., 110, E08001
Owen, T., & Encrenaz, T. 2003, Space Sci. Rev., 106, 121
Owen, T., Mahaffy, P. R., Niemann, H. B., Atreya, S., & Wong, M. 2001, ApJ, 553, L77
Pollack, J. B., Hubickyj, O., Bodenheimer, P., Lissauer, J. J., Podolak, M., & Greenzweig, Y. 1996, Icarus, 124, 62
Terzieva, R., & Herbst, E. 2000, MNRAS, 317, 563
Thode, H. G. 1940, J. Am. Chem. Soc., 62, 581
Tokunaga, A. T., Knacke, R. F., & Ridgway, S. T. 1980, Icarus, 44, 93
Toon, O. B., Turco, R. P., Westphal, D., Malone, R., & Liu, M. S. 1988, J. Atmos. Sci., 45, 2123
Wong, M. H., Mahaffy, P. R., Atreya, S. K., Niemann, H. B., & Owen, T. C. 2004, Icarus, 171, 153
Yung, Y. L., Lee, A. Y. T., Irion, F. W., DeMore, W. B., & Wen, J. 1997, J. Geophys. Res., 102, 10857